PERIÓDICO TCHÊ QUÍMICA
ARTIGO ORIGINAL

METODOLOGIA PARA O CÁLCULO DE PROJETO DE ESTRUTURAS COMPOSITAS DE PAREDES ESPESSAS QUE OPERAM NAS CONDIÇÕES DE CARREGAMENTO EM ALTA VELOCIDADE

DESIGN CALCULATION TECHNIQUE FOR THICK-WALLED COMPOSITE CONSTRUCTIONS OPERATING UNDER HIGH-SPEED LOADING

МЕТОДИКА ПРОЕКТИРОВОЧНОГО РАСЧЕТА ТОЛСТОСТЕННЫХ КОМПОЗИТНЫХ КОНСТРУКЦИЙ, РАБОТАЮЩИХ В УСЛОВИЯХ ВЫСОКОСКОРОСТНОГО НАГРУЖЕНИЯ

BABAYTSEV, Arseniy V.[1*]; RABINSKIY, Lev N.[2];

[1,2] Moscow Aviation Institute (National Research University), Institute of General Engineering Training, Moscow – Russian Federation

** Correspondence author*
e-mail: Ar77eny@gmail.com

Received 03 September 2019; received in revised form 20 October 2019; accepted 26 October 2019

RESUMO

O artigo apresenta uma metodologia para o cálculo da estrutura axissimétrica de paredes espessas, composta por uma barra de aço (componente de reforço) e uma camisa externa de paredes espessas feita de fibra de carbono. A estrutura é carregada com calor linear distribuído ao longo de seu comprimento, associado à pressão externa ativa e forças inerciais. A metodologia baseia-se num modelo unidimensional da barra composta de seção variável levando em consideração as deformações transversais que são necessárias na análise da estrutura de paredes espessas operando sob pressão. Na abordagem proposta, a geometria do produto é dividida em seções e aproximada por fragmentos na forma de cones truncados e, no caso particular, de cilindros. Como resultado dos cálculos, é determinada a distribuição das tensões normais de tração/compressão na carcaça e na haste de reforço, bem como as tensões tangenciais no limite do contato. Como resultado dos cálculos de teste, é mostrada uma consistência bastante boa do modelo unidimensional considerado com modelagem refinada de elementos finitos. Foi estabelecido que a concentração de tensões de cisalhamento é realizada devido à presença de deformações substancialmente não homogêneas nas áreas de mudanças bruscas na geometria, uma redução no raio da casca (aparência de efeitos de arestas) e na área de um aumento acentuado no raio do chanfro da carcaça, onde a pressão externa está no lugar.

Palavras-chave: *estruturas compostas, barra de seção variável, carregamento em alta velocidade, cálculo de projeto, compósito de paredes espessas.*

ABSTRACT

The scientific paper presents a technique for calculating a thick-walled axially symmetrical construction consisting of a steel rod (reinforcing component) and an external thick-walled shell made of carbon fiber. The construction is loaded with linear load distributed along its length, associated with the operating external pressure, and inertial forces. The technique is based on a one-dimensional model of a composite rod of variable cross-section, roughly taking into account transverse deformations, which is necessary when analyzing a thick-walled construction operating under pressure. In the proposed approach, the geometry of the product is divided into sections and approximated by fragments in the form of truncated cones and, in the particular case, in the form of cylinders. As a result of calculations, the distribution of normal tensile/compression stresses in the shell and in the reinforcing rod, as well as tangential stresses at the boundary of their contact, are determined. As a result of test calculations, a fairly good consistency of the considered one-dimensional model with refined finite-element modeling is shown. It has been established that the concentration of shear stresses is realised due to the presence of substantially inhomogeneous deformations in the areas of sharp changes in geometry, a reduction in the radius of the shell (the appearance of edge effects), and in the area of a sharp increase in the radius of the bevel of the shell where external pressure is in place.

Keywords: *composite constructions, variable cross section rod, high-speed loading, design calculation, thick-walled composite.*

DOI: 10.52571/PTQ.v16.n33.2019.495_Periodico33_pgs_480_489.pdf

АННОТАЦИЯ

В работе представлена методика расчета толстостенной осесимметричной конструкции, состоящей из стального стержня (армирующего компонента) и внешней толстостенной оболочки, выполняемой из углепластика. Конструкция нагружается распределенной вдоль ее длины погонной нагрузкой, связанной с действующим внешним давлением, и инерционными силами. Методика основана на одномерной модели составного стержня переменного сечения, приближенно учитывающей поперечные деформации, что необходимо при анализе толстостенной конструкции, работающей под давлением. В предложенном подходе геометрия изделия разбивается на участки и аппроксимируется фрагментами в форме усеченных конусов и, в частном случае, цилиндров. В результате расчетов определяется распределение нормальных напряжений растяжения/сжатия в оболочке и в армирующем стержне, а также касательные напряжения на границе их контакте. В результате тестовых расчетов показана достаточно хорошая согласованность рассмотренной одномерной модели с уточненным конечно-элементным моделированием. Установлено, что концентрация напряжений на сдвиг реализуется из-за наличия существенно неоднородных деформаций в областях резкого изменения геометрии, уменьшение радиуса оболочки (появление краевых эффектов) и в области резкого увеличения радиуса скоса оболочки, где действует внешнее давление.

Keywords: *композитные конструкции, стержень переменного сечения, высокоскоростное нагружение, проектировочный расчет, толстостенный композит.*

1. INTRODUCTION

Design calculations based on one-dimensional approximate models of rods and beams of variable cross section can be effectively used in the development of axially symmetrical constructions of high-fineness ratio. Similar one-dimensional models are used, for example, in the design of columns and supports, including composite ones (Mossakovsky, 1990; Volchkov, 2007; Berezovskii *et al.*, 2015; Dudchenko, 2016; Lomakin *et al.*, 2018a), and (Lurie et al., 2015; Babaytsev *et al.*, 2017; Kakhramanov *et al.*, 2017; Rabinskiy and Tushavina, 2018; Formalev *et al.*, 2018a; Formalev *et al.*, 2018b; Lomakin *et al.*, 2018b; Rabinskiy and Tushavina, 2019a; Formalev and Kolesnik, 2019; Rabinskiy *et al.*, 2019; Nikitin *et al.*, 2019; Rabinskiy and Tushavina, 2019b; Babaytsev *et al.*, 2019). Such models make it possible, at a first approximation, to evaluate the construction strength and determine the loading conditions of its elements (compartments, sections) for further refined numerical calculations. In addition, simplified calculations can be useful for choosing the basic geometric parameters, layout, and structural arrangement of the designed products. Naturally, one-dimensional calculations are not sufficient, even during preliminary design study, but they can be considered basic, reducing the problem to the problem solved by the most simple methods from the structural resistance course (Rabinskiy and Tushavina, 2019c; Babaytsev *et al.*, 2019).

In this scientific paper, we consider the task of designing a composite axially symmetrical product consisting of a steel cylindrical rod (reinforcing component) located in the central part and a thick-walled shell surrounding it, made of carbon fiber and having an external diameter that varies along the axis of the product (see Figure 1). Intensive pressure having an effect on the outer surface of the shell in the rear part of the construction leads to large accelerations in the axial direction and, accordingly, to large values of inertial loads (Mykhalevskiy, 2018; Akbarov *et al.*, 2018; Mykhalevskiy and Horodetska, 2019). As a result, the construction operates under difficult stress conditions (all-round compression in the rear part, longitudinal compression in the front part, shear at the contact boundary of the shell and the rod, and in the region of change in the cross-section of the shell, etc.), which, however, at a first approximation, can be reduced to a simple one-dimensional case of loading a variable cross section composite rod (Dmitriev *et al.*, 2011; Skvortsov *et al.*, 2000). The task of the calculation in such a simplified model is to determine the tensile/compression stresses in the shell and in the rod, as well as to determine the tangential stresses in the zone of their contact (Yasnitskii, 1989; Gorchakov *et al.*, 2004; Skvortsov *et al.*, 2012). To assess the strength and integrity of the construction, the found stresses are compared, respectively, with the tensile strength of the shell material, the yield strength of the metal rod and the shear strength (resistance of collapse) of their contact joint.

A distinctive feature of the calculations is the relatively small aspect ratio of the products under consideration and the presence of

significant external pressure. In this case, neglecting the transverse deformations of the composite shell in the radial and circumferential directions leads to significant calculation errors. To take these deformations into account, at a first approximation, we use the technique proposed in (Kornev *et al.*, 2018), in which, practically, one can use the solution of the Lamé problem on deformations of a thick-walled hollow cylinder under pressure (Sedov, 1970). Initially, in (Kornev *et al.*, 2018), calculations were carried out only for the endings of the construction under consideration. In this work, the technique (Kornev *et al.*, 2018) is generalized to the case of an arbitrary number of sequentially arranged compartments of a given conical or cylindrical shape, for which a solution is framed taking into account the matching conditions at the boundaries of their contact. Since the geometry of the compartments is known in the case under consideration, the solution can be framed using the integral form of the equilibrium equations for each compartment of the product, in contrast to (Kornev *et al.*, 2018), where the equilibrium equations in differential form were used. The reliability of the proposed technique for design calculations is verified by the example of the typical geometry of the product under consideration, for which precise numerical calculations by the finite element method are carried out.

Note that in the model used, only the longitudinal characteristics of the product materials are available, therefore, in the general case, the technique turns out to be fair for both isotropic and anisotropic composite materials of the shell. The manufacturing technology of the shell is also insignificant, and it can be performed, for example, in the form of a thick-walled layered composite or by winding, etc.

2. MATERIALS AND METHODS

We consider an axially symmetrical composite construction in the form of a cylindrical steel rod and an external composite shell of variable cross section (see Figure 1). The structure is loaded with an external pressure p having an effect on the surface of the rear conical part of the shell (see Figure 3a). The pressure leads to an all-round compression of the rear part of the product, and its projection onto the central axis leads to the acceleration of the construction in the longitudinal direction a and to the corresponding inertial loads. Provided that the rod can be slightly longer than the shell, this can be taken into account by attaching the masses m0 and m1 at the front and rear ends of the rod.

2.1. Acceleration of the product and average shear stresses on the thread

First of all, we determine the acceleration of the product at a given pressure. If we know the whole mass of the product *m* (the shell, the rod and, if there are attached masses) and the maximum cross-sectional area of the rear part of the product *S*, which is under pressure, will be found Equation 1. Further, at a "zero-order" approximation, we estimate the shear linear force having an effect in the direction of the axis of the rod in the region of the threaded contact with the shell. We replace the impact of the shell on the rod by a distributed linear force $\overline{T}$ constant in magnitude (this is the main simplification at this stage of calculating the "zero-order" approximation) and having an effect in the longitudinal direction. By writing down the equation of equilibrium for the rod as a solid body, we find (Equation 2). Where m_c – the mass of the rod, Equation 3 – the cross-sectional area of the rod, ρ_c _ the density of the rod material, L – the length of the rod and Equation 4 – the diameter of the rod.

Then crosscutting linear effort is determined from the following Equation 5. The average tangential stresses on the thread are determined from the ratio (Equation 6).

2.2. Model of the integral composite rod

To frame a solution at a first approximation, we shall frame a solution in a one-dimensional setting, considering the equilibrium of the product only in the direction of its axis of symmetry. To do this, we integrate all the acting loads by the cross section and by the outer surface of the product, and remove them to the central axis. At a first approximation, we assume that all stresses are constant by the cross section of the shell and the rod. This approach allows us to evaluate the normal tensile/compression stresses in the outer shell $\sigma_0(z)$ and in the rod $\sigma_c(z)$, as well as tangential stresses at the boundary of their contact $\tau(z)$. The outer duct of the real product is approximated by piecewise linear sections, that is, the axially symmetrical geometry of the shell is approximated by sections in the form of truncated cones and cylinders. The

rod is modeled as a cylinder. It is assumed ideal contact between the rod and the shell.

In order to frame a solution, let us consider the truncated part of the product fragment presented in Figure 2. This figure shows the external loads and internal stresses having an effect on the truncated fragment of the shell and the rod (shown by hatching). We write down the equations of equilibrium and strain compatibility conditions for *i*-th product fragment within which the axial coordinate varies in the range $z_{i-1} \le z \le z_i$. We obtain the following ratios:

1) The equilibrium condition of the outer shell element (Equation 7). Where Equation 8 – the cross-sectional area of the considered *i*-th element of the shell at the point *z,* Equation 9 – the radius of the cross section of the fragment at a given point, $R_i(0)$ – the radius of the initial section of the fragment, α_i – taper angle of the fragment (for cylindrical fragments α_i = 0, $\sigma_0(z)$ – stresses in the current section of the shell fragment, $\sigma_0(z_{i-1})$ – stresses having an effect on the left boundary of the shell fragment under consideration (at the initial point *z* = 0, these stresses are equal to the operating pressure *p*, and then they are determined based on the solution in the previous section of the product), Equation 10 – the volume of the shell fragment, Equation 11 – the volume of the rod fragment, Equation 12 – the resultant of shear stresses having an effect on the contact of the shell fragment and the rod.

2) The equilibrium condition of the rod element is determined using Equation 13. Where Equation 14 – the cross-sectional area of the rod; and at the starting point, the stresses are calculated taking into account the operating pressure and the mass attached (Equation 14).

3) strain compatibility conditions with approximate allowance for the operating pressure are written as follows (Equation 15) (Kornev *et al.*, 2018). Where E_s, E_o, ν_s, ν_o – elastic moduli and Poisson's ratios of the materials of the rod and the shell, respectively.

For the shell fragments on which pressure does not have an effect Equation 7 reduces to a simpler ratio (Equation 16), which determines the equality of longitudinal deformations in the rods and in the shell. A detailed derivation of the ratio (Equation 7) was presented in (Kornev *et al.*, 2018) based on the solution of the Lamé problem for a thick-walled cylinder loaded with pressure.

From the written down three Equations 7 – 17, three unknown functions are determined: $\sigma_0(z)$, $\sigma_c(z)$, $T(z)$. The tangential stresses at the contact of the rod and the shell are determined from the Equation 18.

These stresses, in contrast to the solution of the "zero" approximation (Equation 6), turn out to be variable by the length of the rod. The found stress values are compared with the corresponding maximum permissible stresses for the materials of the shell, the rod and their threaded connection.

3. RESULTS AND DISCUSSION:

3.1. Initial data

We consider an example of product geometry presented in Figure 3. The total length of the product is 500 mm. The maximum cross-sectional diameter d_{max} = 160 mm, and its area, respectively (Equation 19). The diameter of the reinforcing rod is 20 mm. Operating pressure *p* = 300 MPa. The rod material is steel with properties ρ_s = 7850 kg/m^3, E_s = 200 GPa, ν_s = 0.3. Yield strength of steel under tension and compression σ_s =±355 MPa. The material of the composite shell is carbon laminate with a density ρ_o = 1500 kg/m^3 and with characteristics in the direction of the product axis E_o = 60 GPa, ν_o = 0.35, σ_o = +1100/-700 MPa. The shear strength (resistance of collapse) of the joint is 120 MPa. Attached masses at the ends of the rod are absent. The total mass of the construction *m* = 4.47 kg.

On the basis of (Equation 1) we find the acceleration of the product for the given conditions of the problem *a* = 1.341 m/s. This acceleration is quite large, however, it is less than the speed of sound in the materials under consideration, therefore, at a first approximation, all calculations, including numerical ones, can be carried out in a quasi-static setting. The average tangential shearing stress is determined from (Equation 6) and is $\overline{\tau} = 114$ MPa. Thus, from a simple design calculation of the "zero" approximation, it follows that the strength margin of the joint under given loading conditions can be quite large (more than 114.3 MPa), if, due to the optimal choice of the product geometry, an approximately constant shear force along the length of the rod can be realized. Structural failure can occur only due to the uneven distribution of shear forces, that is, the presence of a concentration of shear stresses on the mount, which can be associated, for example,

with a sharp change in the size of the cross section of the outer shell.

3.2. Numerical modeling

To verify the results of design calculations, we will carry out numerical modeling applying the finite element method with the use of Ansys Workbench software, taking into account the axial symmetry of the problem. An example of a finite element model of the product is shown in Figure 3. The average size of the elements is ~ 1.5 mm; the total number of elements in the model is ~ 16274. The pressure is set in the region of the rear part of the product (at the border highlighted in color in Figure 3) and is balanced by the inertial forces associated with acceleration in the longitudinal direction of the product. The threaded connection is not drawn – an ideal contact is set between the rod and the shell along a smooth boundary, remote from the central axis by a distance equal to the radius of the rod. The calculation is carried out in a linearly elastic setting under the assumption of small strains, at the quasi-static approximation. The results of numerical modeling are presented in Figure 4. It shows the distribution of normal stresses in the longitudinal direction and tangential stresses in the plane of the model section (*zr).*

3.3. Comparison of analytical and numerical calculations

Figure 5 shows a comparison of the results of design calculations by the analytical method described in section 2.2., with the results of numerical modeling presented in section 3.2. It shows the distribution of normal stresses in the longitudinal direction in the rod (on the central axis) and in the shell. The distribution of tangential stresses at the contact boundary of the shell and the rod is shown in Figure 5c.

From the calculation results it follows that the concentration of shear stresses is realized due to the presence of substantially inhomogeneous strains in the areas of sharp changes in geometry, a decrease in the radius of the shell (the emergence of edge effects), and in the region of a sharp increase in the radius of the bevel of the shell, where external pressure has an effect. In these places, a fastener cut may begin. This can be eliminated by strengthening these areas, in particular, by increasing the radius. The estimation by the model of the integral composite rod (see section 2.2), gives significant errors, although the found value of 390 MPa approximately corresponds to the level of effective stresses. Normal stresses turns out to be negative along the entire length of the rod and in the shell in front part of the product. Positive tensile stresses are realized in the shell material in the rear part of the product, where external pressure has an effect. These stresses *exceed* the specified tensile strengths of materials.

The obtained analytical solution is quite close to the results of numerical modeling. It can be seen that the tangential force in the analytical solution is overestimated in the concentration region, and thus designing on the basis of this solution provides an additional margin of safety for the joint. This approximate solution can be used for preliminary product design and for choosing the geometry of the outer shell, which provides shear strength of the fastener and tensile-compressive strength of the rod and the shell without taking into account the concentration associated with the uneven distribution of stresses over the shell cross section (see Figure 5).

In general, further consideration requires an improved three-dimensional calculation with layered analysis. And speaking of composites – it is necessary to take into account the complex criteria of a combined stress, layer-by-layer analysis.

4. CONCLUSIONS:

1. The technique for calculating a thick-walled axially symmetrical construction has been considered.

2. A one-dimensional model of a composite rod of variable cross section, approximately taking into account transverse strains, was regarded. As a result of calculations, the distribution of normal tensile/compression stresses in the shell and in the reinforcing rod, as well as tangential stresses at the boundary of their contact, are determined.

3. As a result of test calculations, a fairly good consistency of the considered one-dimensional model with improved finite-element modeling is shown. Normal stresses in the longitudinal direction and tangential stresses in the plane of the model section under consideration were obtained using the described technique and the finite element method. A comparative analysis of the results obtained was carried out. Recommendations are given for further consideration of such constructions.

5. ACKNOWLEDGMENTS:

The work was carried out with the financial support of the state project of the Ministry of Education and Science project code 2.9219.2017/8.9.

6. REFERENCES:

1. Akbarov, R.D., Zhilisbaeva, R.O., Tashpulatov, S.S.H., Cherunova, I.V., Bolysbekova, R.T. I*zvestiya Vysshikh Uchebnykh Zavedenii, Seriya Teknologiya Tekstil'noi Promyshlennosti*, 2018, 2018-January(5), 188-192
2. Babaytsev, A., Dobryanskiy, V., Solyaev, Y. *Lobachevskii Journal of Mathematics*, **2019**, *40*(7), 887-895. DOI: 10.1134/S1995080219070059.
3. Babaytsev, A.V., Prokofiev, M.V., Rabinskiy, L.N. *International Journal of Nanomechanics Science and Technology,* **2017**, *8*(4), 359-366. DOI: 10.1615/NanoSciTechnolIntJ.v8.i4.60.
4. Berezovskii, V.V., Shavnev, A.A., Solyaev, Y.O., Lur'e, S.A. *Russian Metallurgy (Metally)*, **2015**, *10*, 790-794.
5. Dmitriev, A.I., Skvortsov, A.A., Koplak, O.V., Morgunov, R.B., Proskuryakov, I.I. Physics of the Solid State, **2011**, *53*(8), 1547-1553.
6. Dudchenko, A.A. Calculation, design and manufacturing technology of thermostable composite rod. *Composite Materials Constructions*, **2016**, *1*, 3-11.
7. Formalev, V.F., Kolesnik, S.A. *Journal of Engineering Physics and Thermophysics*, **2019**, *92*(1): 52-59.
8. Formalev, V.F., Kolesnik, S.A., Kuznetsova, E.L. *Periodico Tche Quimica*, **2018a**, *15*(Special Issue 1), 426-432.
9. Formalev, V.F., Kuznetsova, E.L., Kuznetsova, E.L. *Periodico Tche Quimica*, **2018b**, *15*(Special Issue 1): 377-389.
10. Gorchakov, A.I., Semenova, A.V., Syrovatskaya, Yu.V., Shcherbakov, Yu.V., Yasnitskij, L.N. *Fizika i Khimiya Obrabotki Materialov*, **2004**, *1*, 43-47.
11. Kakhramanov, R.M., Knyazeva, A.G., Rabinskiy, L.N., Solyaev, Y.O. *High Temperature*, **2017**, *55*(5), 731-736.
12. Kornev, Yu.V., Emelyanov, S.V., Lukyanova, A.Yu., Semenov, N.A., Semenov, P.E., Babaytsev, A.V. *Composites: Mechanics, Computations, Applications*, **2018**, *9*(4), 283-295. DOI: 10.1615/CompMechComputApplIntJ.2018025142.
13. Lomakin, E., Rabinskiy, L., Radchenko, V. *Meccanica*, **2018a**, *53*(15), 3831-3838. DOI: 10.1007/s11012-018-0919-y.
14. Lomakin, E.V., Lurie, S.A., Belov, P.A., Rabinskiy, L.N. *Doklady Physics*, **2018b**, *63*(12), 503–507.
15. Lurie, S.A., Kuznetsova, E.L., Rabinskiy, L.N., Popova, E.I. *Mechanics of Solids*, **2015**, *50*(2), 135-146.
16. Mossakovsky, V.I. *The strength of rocket structures,* Moscow: Vysshaya shkola, **1990**.
17. Mykhalevskiy, D. *Eastern-European Journal of Enterprise Technologies,* **2018**, *6*(9-96), 16-21
18. Mykhalevskiy, D.V., Horodetska, O.S. *Journal of Mechanical Engineering Research and Developments*, **2019**, *42*(2), 2019, 50-57
19. Nikitin, P.V., Tushavina, O.V., Shkuratenko, A.A. *Incas Bulletin*, **2019**, *11*(Special Issue), 191-201. DOI: 10.13111/2066-8201.2019.11.S.19.
20. Rabinskiy, L.N., Tushavina, O.V. *Incas Bulletin*, **2019a**, *11*(Special Issue), 203-211. DOI: 10.13111/2066-8201.2019.11.S.20;
21. Rabinskiy, L.N., Tushavina, O.V. *Periodico Tche Quimica*, **2018**, *15*(Special Issue 1), 321-329.
22. Rabinskiy, L.N., Tushavina, O.V., Fedotenkov, G.V. *Asia Life Sciences*, **2019b**, Supplement 19(1), 49-162.
23. Rabinsky, L.N., Tushavina, O.V. *STİN*, **2019c**, *4*, 22-26.
24. Sedov, L.I. *Continuum Mechanics*, Moscow: Nauka, **1970**.
25. Skvortsov, A.A., Orlov, A.M., Frolov, V.A., Gonchar, L.I., Litvinenko, O.V. *Physics of the Solid State*, **2000**, *42*(10), 1861-1864.
26. Skvortsov, A.A., Orlov, A.M., Zuev, S.M. *Russian Microelectronics*, **2012**, *41*(1), 31-40.
27. Volchkov, O. D. *The strength of launch*

vehicles. Moscow: MAI Publishing House, **2007**.
28. Yasnitskii, L.N. *Mechanics of Solids*, **1989**, *24*(2), 90-96.

$$a = pS/m \quad \text{(Eq. 1)}$$

$$m_c a = pS_c + \bar{T}L \quad \text{(Eq. 2)}$$

$$S_c = \pi d_c^2 / 4 \quad \text{(Eq. 3)}$$

$$d_c = 2R_c \quad \text{(Eq. 4)}$$

$$\bar{T} = \left(m_c a - pS_c\right)/L \quad \text{(Eq. 5)}$$

$$\bar{\tau} = \frac{\bar{T}}{2\pi R_c} \quad \text{(Eq.6)}$$

$$\sigma_0(z)S_i(z) = \sigma_0(z_{i-1})S_i(z_{i-1}) + \rho_0 a V_i(z) + T(z) - p\left(S_i(z) - S_i(z_{i-1})\right) \quad \text{(Eq. 7)}$$

$$S_i(z) = \pi\left(R_i^2(z) - R_p^2\right) \quad \text{(Eq. 8)}$$

$$R_i(z) = R_i(0) + \left(z - z_{i-1}\right)\tan\alpha_i \quad \text{(Eq. 9)}$$

$$V_i(z) = \frac{1}{3}\pi\left(z - z_{i-1}\right)\left(R_i^2(0) + R_i(0)R_i(z) + R_i^2(z)\right) - V_c(z) \quad \text{(Eq. 10)}$$

$$V_c(z) = \pi R_p^2\left(z - z_{i-1}\right) \quad \text{(Eq. 11)}$$

$$T(z) = 2\pi R_c \int_{z_{i-1}}^{z} \tau(x)dx \quad \text{(Eq. 12)}$$

$$\sigma_c(z)S_c = \sigma_c(z_{i-1})S_c + \rho_c a V_c(z) - T(z) \quad \text{(Eq. 13)}$$

$$S_c = \pi R_c^2 / \quad \text{(Eq. 14)}$$

$$\sigma_c(0) = \frac{m_0 a}{S_c} - p \quad \text{(Eq. 15)}$$

$$E_c\sigma_0 = E_0\sigma_c \quad \text{(Eq. 16)}$$

$$\sigma_0(z) = \frac{E_0}{E_c}\left(\sigma_c(z) + 2\nu_c p\right) - 2\nu_0 p \quad \text{(Eq. 17)}$$

$$\tau(z) = \frac{d}{dz}\left(\int_{z_{i-1}}^{z} \tau(x)dx \right) = \frac{1}{2\pi R_c} \frac{dT(z)}{dz} \qquad \text{(Eq. 18)}$$

$$S = \frac{\pi \cdot d_{\max}{}^2}{4}. \qquad \text{(Eq. 19)}$$

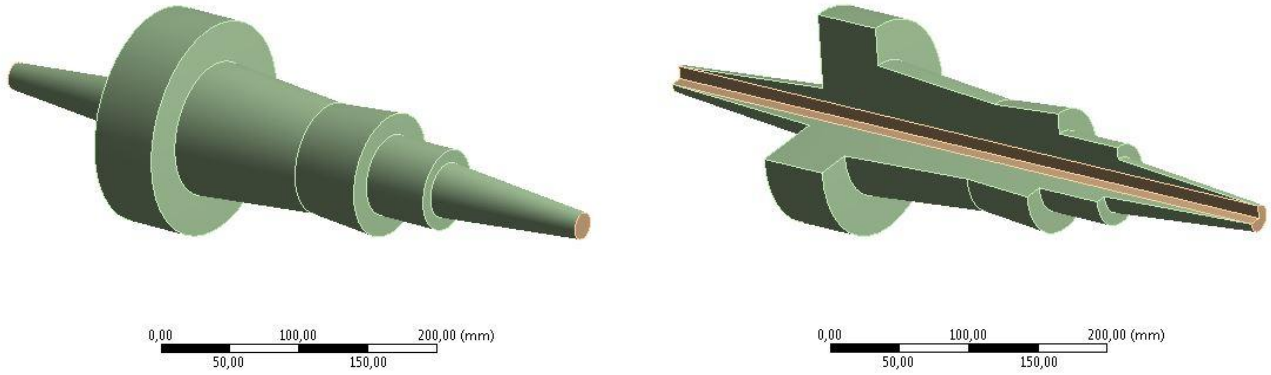

Figure 1. *Integral composite rod: 1 – steel reinforcing component, 2 – external composite shell of variable cross section*

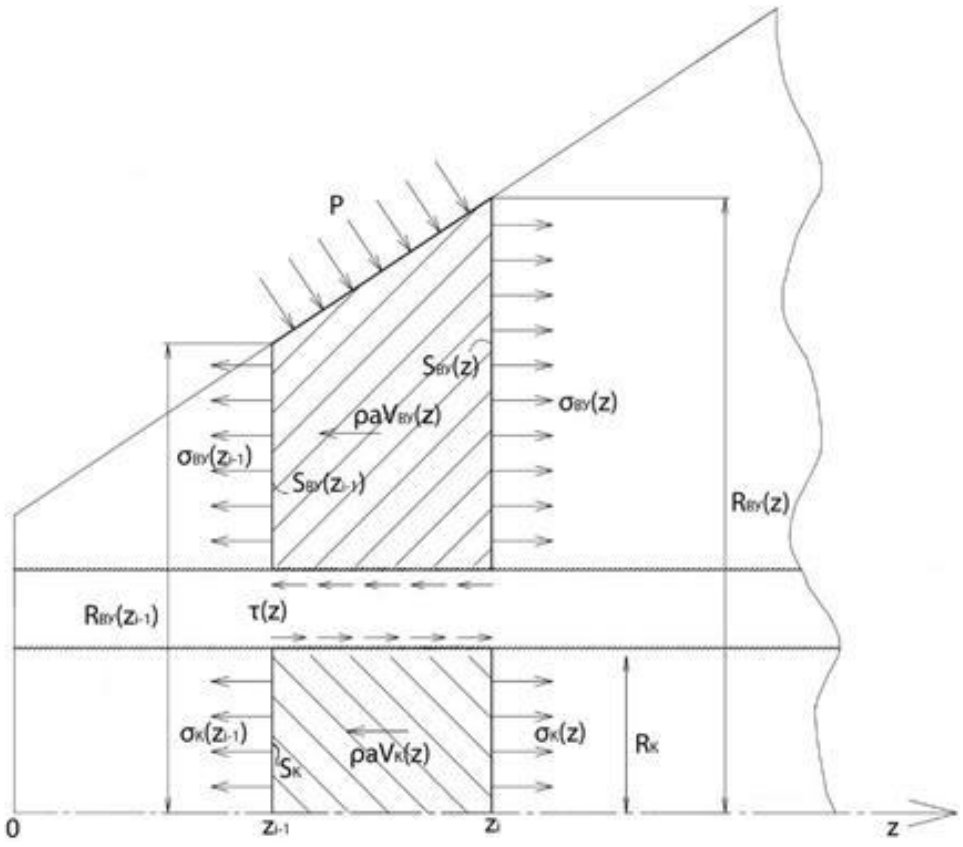

Figure 2. *Fragment of the rod and the outer shell, and the loads having an effect on them*

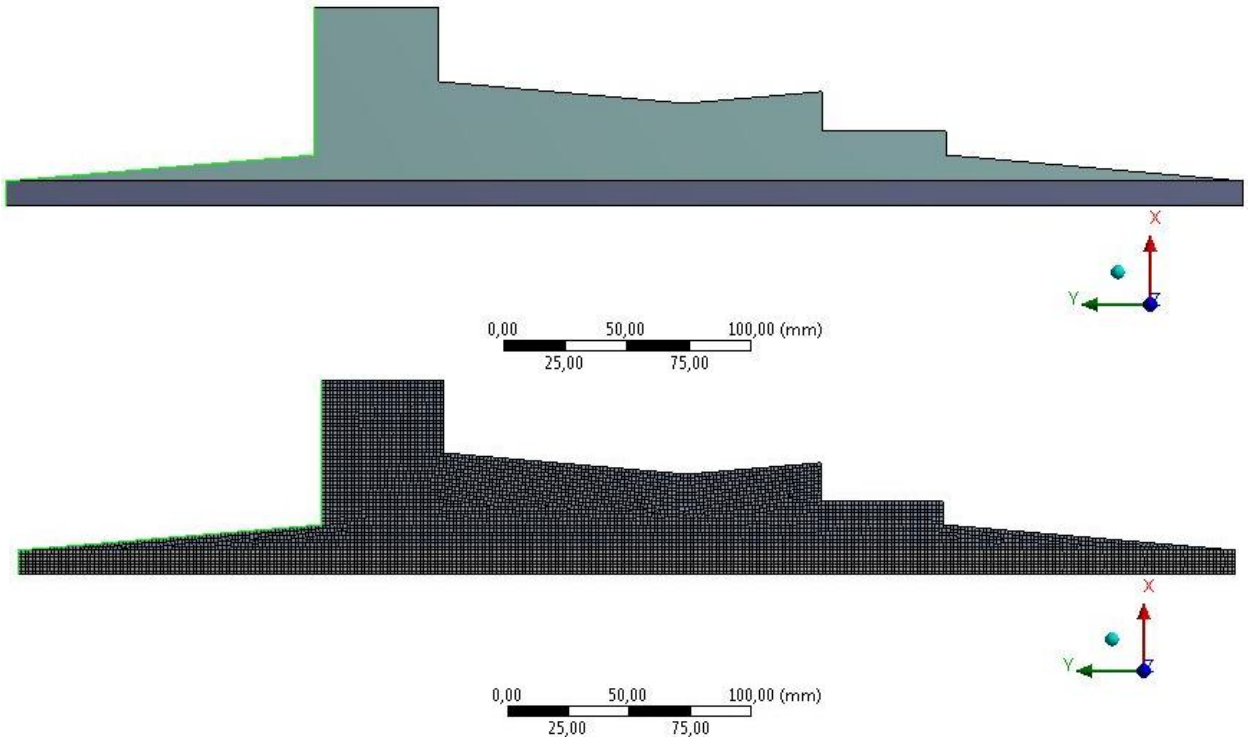

Figure 3. *An example of the considered geometry of the product and its finite element model. The zone of external pressure effect is shown in color*

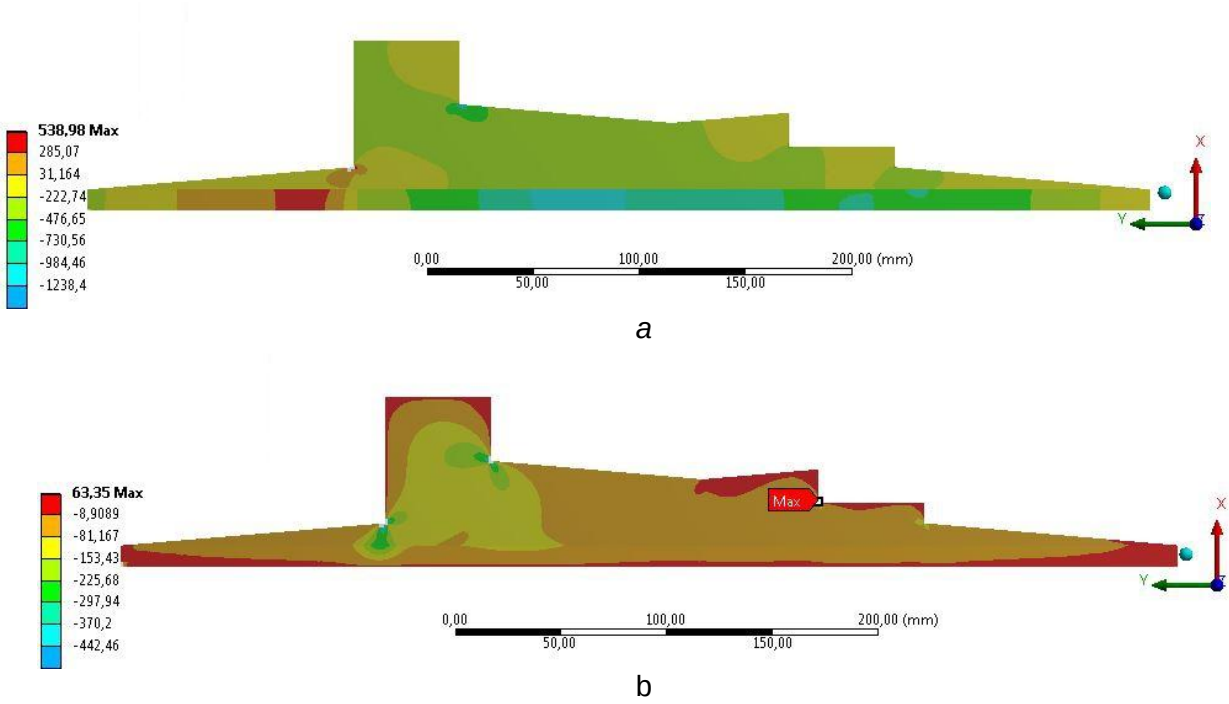

Figure 4. *The results of finite element modeling, a: normal stresses in the longitudinal direction, b: tangential stresses in the plane of the considered model section*

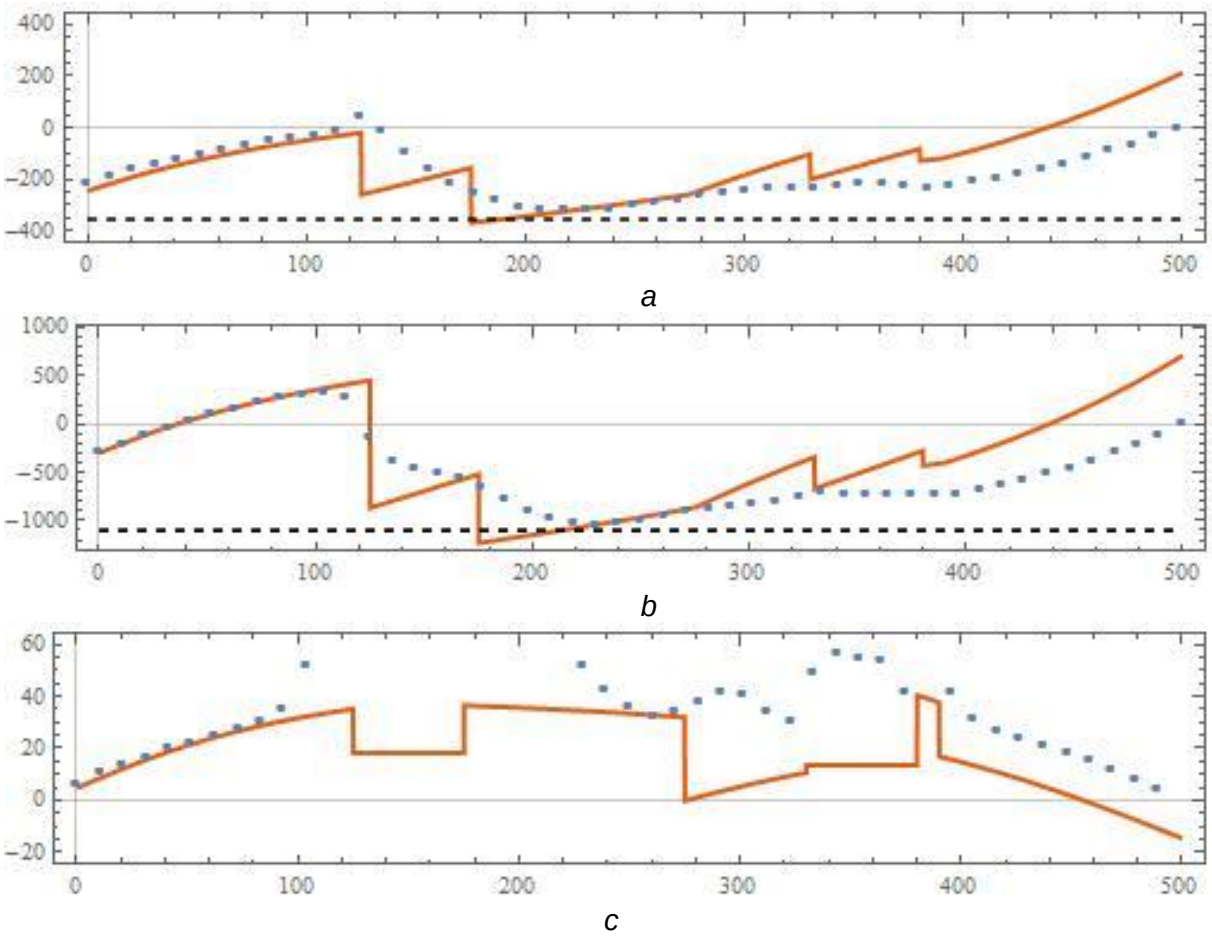

Figure 5. *Comparison of the results of analytical (solid lines) and numerical (points) modeling, a: longitudinal stresses in the rod Sc(z) [MPa], b: longitudinal stresses in the shell So(z) [MPa], in: tangential stresses at the contact τ(z) [MPa]. Dotted lines show the corresponding stress limits*